Brazilian Journal
of Chemical
Engineering

ISSN 0104-6632
Printed in Brazil
www.abeq.org.br/bjche

Vol. 31, No. 01, pp. 57 - 68, January - March, 2014

NON-WOVEN NANOFIBER CHITOSAN/PEO MEMBRANES OBTAINED BY ELECTROSPINNING

M. T. M. Bizarria[1], M. A. d'Ávila[2] and L. H. I. Mei[1*]

[1]School of Chemical Engineering, State University of Campinas, UNICAMP, Campinas - SP, Brazil.
[2]Department of Materials Engineering, School of Mechanical Engineering, State University of Campinas, UNICAMP, Campinas - SP, Brazil.
E-mail: lumei@feq.unicamp.br

(Submitted: June 17, 2012 ; Revised: February 4, 2013 ; Accepted: March 11, 2013)

Abstract - The present work focused on the preparation and morphological characterization of chitosan-based nanofiber membranes, aiming at applications in medical and pharmacological areas. Membranes with nanofiber diameters ranging from 50 – 300 nm were prepared from polymer solutions through the electrospinning process. To stabilize the process, it was necessary to use poly(ethylene oxide) (PEO), which is a biocompatible synthetic polymer. Pure chitosan solutions, as well as chitosan and PEO solution blends, were characterized by their rheological behavior, conductivity, and surface tension measurements. The electrospun fiber thermal characteristics and crystalline structures were investigated through thermogravimetric analysis (TG) and differential scanning calorimetry (DSC). Scanning electron microscopy images (SEM) were used for the morphological evaluations of the membranes. The addition of PEO to the chitosan solutions improved their electrical conductivity, surface tension and viscosity, greatly favoring the electrospinning process. Thus, membranes with 80% chitosan could be electrospun.
Keywords: Electrospinning; Nanofibers; Biocompatible-membranes; Chitosan; PEO.

INTRODUCTION

In the field of nanotechnology, obtaining fibers with characteristic diameters in the range of 100-200 nm from both natural and synthetic biocompatible polymers, known as nanofibers, has proven to be a promising area for applications in the medical and pharmaceutical fields. Due to their broad surface area, they present improved mechanical properties, as well as features to obtain different morphologies and geometries, allowing for applications in different technological fields such as filtration, multi-functional membranes, tissue engineering, wound dressing, controlled drug release, scaffolds and vascular prostheses (Huang *et al*., 2003; Wu *et al*., 2006; Ramakrishna *et al*., 2005; Ma *et al*., 2005; Schindler *et al*., 2005; Jayakumar *et al*., 2010).

Among the different technologies that have been applied to obtain nanofibers, the electrospinning technique is highlighted, since it is a low-cost and versatile technique that allows fiber preparation in the nanometer and submicrometer ranges (Zhou and Gong, 2008). This method was successfully applied in a great variety of polymeric systems, in which nanofibers with different sizes and morphologies were reported (Ramakrishna *et al*., 2005).

The nanofiber production mechanism occurs due to the electrostatic forces acting in a viscous polymeric solution through the application of a strong electric field between a grounded target and a poly-

*To whom correspondence should be addressed

mer solution. In its simplest version, the electrospinning-process setup consists of a syringe, to hold the polymer solution, coupled to a stainless steel needle used as a conducting capillary, a high voltage power supply, two electrodes and a grounded surface collector. The polymer solution should just drip from the needle tip (generally at 0.1-1.5 mL/h). The process is initiated when an electric field is generated by the high-voltage power supply (in the range of 5 to 30 kV) between the conducting capillary and the grounded collecting surface. When the applied voltage is high enough to overcome the polymer-solution drop surface tension, one or more electrically charged jets are created and usually become unstable, acquiring spiraled shapes. The jets continue drying and whipping to form very thin fibers until they are collected on the grounded collector, forming a non-woven web.

Although apparently simple, the process requires strict control of the variables essential to obtain nanometric fibers with good uniformity. In natural polymer electrospinning, the fibers are produced from a polymeric solution. Therefore, variables such as solution concentration, viscosity, electrical conductivity and surface tension should be established to guarantee a successful operation. Additionally, process parameters such as electric field intensity, flow rate, distance between the capillary and the collector, fiber-collection method, temperature and humidity should be established (Huang *et al*., 2003; Ramakrishna *et al*., 2005; Li *et al*., 2005; Zhou and Gong, 2008; Jayakumar *et al*., 2010).

In applications in the medical and pharmaceutical fields, nanofibers must be prepared using biocompatible polymers, which can be either of a synthetic or natural renewable origin. Among the synthetic-origin polymers, those such as poly(ethylene oxide) (PEO), poly(vinyl alcohol) (PVA) and poly(caprolactone) (PCL) are often cited in literature, while poly(L-lactic acid) (PLLA), cellulose and its derivatives, as well as chitin and chitosan, are among the most studied natural renewable-origin polymers (Ramakrishna *et al*., 2005; Sajeev *et al.,* 2008).

Synthetic fibers tend to present superior mechanical properties such as tensile strength and modulus when compared to natural fibers. Besides, they have the advantage of being more suitable for processing and do not require purification procedures, which are necessary in some natural polymeric systems (Teo and Ramakrishna, 2006; Kumbar *et al*., 2008; Sajeev *et al*., 2008). On the other hand, natural systems usually present multifunctional bioactive properties that grant them superior performance in biological environments due to their higher biocompatibility (Petrulyte, 2008). These polymers provide better interaction with the human body, rendering systems of interest for new applications in medical and biological fields.

One of the main natural polymers currently researched is chitosan. This polymer is obtained through partial chitin deacetylation, being an attractive material for medical applications due to its biodegradability, anti-fungal action**,** wound-healing effects and immunological-system stimulation (Silva *et al*., 2006).

In this work, the results of the electrospinning of chitosan/PEO blends in different processing conditions are presented. Blend-solution rheological properties, electrical conductivities and surface tensions were determined. Fiber morphologies and diameters were analyzed using scanning electron microscopy (SEM), while thermal analyses, such as thermogravimetry (TG) and scanning differential calorimetry (DSC), were performed to investigate any possible change in the thermal properties compared to the original polymers.

EXPERIMENTAL

Materials

Chitosan, with a medium molecular weight (MMW), (284cP, 1%wt chitosan in 1% acetic acid) and 80% deacetylation degree (DD), was obtained from Aldrich. Sodium chloride (NaCl), PA-ACS, and glacial acetic acid, PA-ACS, were obtained from Synth; poly(ethylene oxide) (PEO), with a molecular weight of 900,000 g/mol, was obtained from Aldrich. All materials were used as received. Deionized water was used to prepare the solutions.

Equipment

The electrospinning equipment, built by our research group, consists of a high-voltage power supply with controlled tension values ranging from 2 to 32 kV and a solution-contention system composed of a 10 mL syringe coupled to a stainless steel needle with a 1 mm internal diameter. The solution flow rate was established by the pressure drop due to gravity. The electrospun fibers were collected with a grounded aluminum plate or grounded 80-rpm rotating stainless-steel drums with outer diameters of 32 or 2.2 mm. Both electrospinning equipment schemes used in this work are shown in Figure 1.

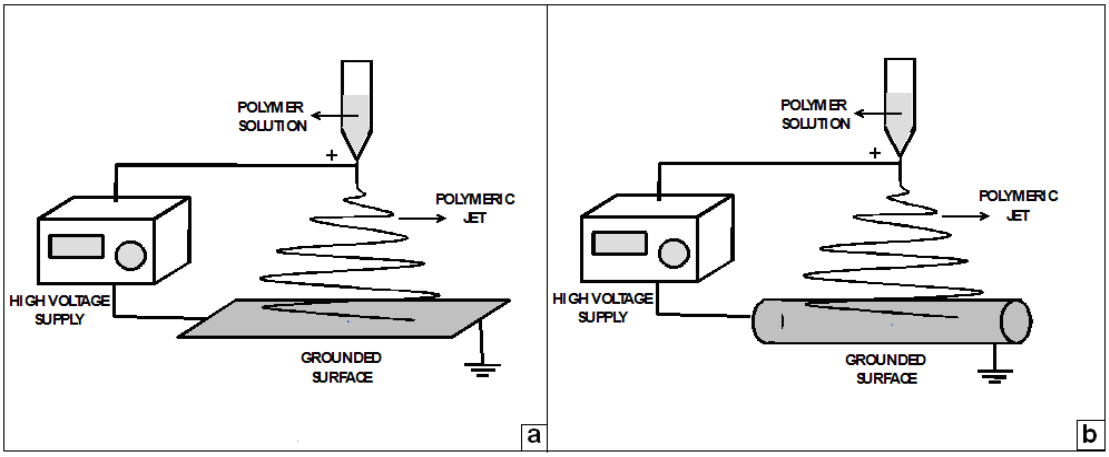

Figure 1: Scheme of the basic electrospinning apparatus: a) with a grounded aluminum plate as a collector; (b) with a grounded 32mm diameter rotating device as a collector.

Chitosan Solutions

MMW chitosan solutions with different concentrations were prepared using as solvent an aqueous solution 90% v/v of acetic acid. Chitosan (powder) was weighed and the solvent was also added by weight to reach final concentration solutions of 1, 2, 4, 6, and 7% (w/w). The mixtures were left under continuous agitation with magnetic stirrers for at least two days. All solutions used in the present work are summarized in Table 1.

Table 1: Chitosan solutions.

(%) Chitosan	Chitosan weight (g)	90% acetic acid solution weight (g)	Amount prepared (g)
1	0.25	24.75	25
2	0.50	24.50	25
4	2.00	48.00	50
6	3.00	47.00	50
7	1.75	23.25	25

Chitosan/PEO Blend Preparations

Chitosan/PEO blends were prepared from the initial 4, 6 and 7% chitosan solutions (see Table 1) using an aqueous 3% (w/v) PEO solution. Additionally, blends containing 1% NaCl in relation to the chitosan solution were also prepared. All blends were prepared with a minimum of two hours of agitation on a magnetic stirrer at room temperature and are summarized in Table 2.

In order to obtain membranes composed of submicron/nanometric nonwoven fibers, the chitosan/PEO blends were submitted to electrospinning and the processing parameters were evaluated. The feed flow rates were dependent on the solution viscosity and ranged from 0.5 to 1.5 mL/h and electric fields between 2 to 3 kV/cm were estimated by using the values of the applied voltage of 20 kV and a range of distance of 7-10 cm from the capillary to the collecting plate. Temperature and relative humidity readings remained between 23 and 26 °C and 34 and 44%, respectively.

Table 2: Preparation of the blends and membrane compositions

Samples			NaCl* (%)	Amount of chitosan solution (g)	Amount of 3% w/v PEO solution (ml)	Final chitosan % in the membrane	Final PEO % in the membrane
Chitosan solution	Electrospun Solution or blend	Ratios of the chitosan/PEO solutions					
4%	4A	3/0	0	(Pure)	zero	100	zero
	4B	3/1	0	30.00	10.0	80	20
	4C	3/1	1	30.00	10.0	67	17
6%	6A	2/0	0	(Pure)	zero	100	zero
	6B	2/1	0	40.00	20.0	80	20
	6C	2/2	0	30.00	30.0	67	33
	6D**	2/2	1	30.00	30.0	60	30
7%	7A	1/1	0	10.00	10.0	70	30

* % relative to chitosan solution.
**the same blend 6C (added salt after preparation).

Electrospinning

Chitosan Solution and Blend Characterizations

Solutions and blends were characterized by measuring their surface tension, viscosity as a function of the shear rate and electric conductivity. Surface tension measurements were performed using a KSV-Sigma 701 tensiometer, by the plate method, at a speed of 2 mm/min and 40% relative humidity. Viscosities, as a function of the shear rate, were measured using a HAAKE- Rheostress 1 rheometer with the parallel plate method at room temperature. The shear rate ranged from 0.1 to 100 s^{-1}. Electrical conductivity was evaluated using a Digimed-DM32 bench conductivity meter, with a conductivity cell K=1 cm^{-1} in the range of 0.01 μScm^{-1} to 2 Scm^{-1}, a 0.1 / 0.01 / 0.001 interchangeable resolution and 0.05% relative precision.

Electrospun Membrane Characterizations

Scanning Electron Microscopy (SEM)

SEM images were obtained using a high resolution SEM, mod. LEO 440i, with an accelerating voltage of 20 kV and 50 pA. Before the SEM analysis, the samples were coated with a thin layer of gold by sputtering to improve their conductivity. The fiber diameters were obtained from the image using the software Image Tool.

Membrane Porosity

Three disks of 20 mm diameter of each membrane examined were weighed and placed in individual glass vials containing absolute ethyl alcohol to allow for diffusion into the empty spaces of the specimens. They were left to stand for 36 hours and transferred into a platform shaker at 100 rpm at room temperature for 3 hours. Then the specimens were removed and placed on paper tissues to extract excess liquid and weighed again. The estimated membrane porosities, expressed as percentage, were calculated using the following equation: P= [VEtOH /(VEtOH + VMEMB)].100, where: P is the estimated porosity of each membrane analyzed (as a percentage of empty space) and V_{EtOH} is the ratio between the observed mass change (after and before the liquid intrusion) and the absolute ethyl alcohol density. Finally, V_{MEMB} is the ratio between the disk initial mass before intrusion and the membrane density. The membrane density can be determined by the method of gradient column.

Thermal Characterization

TG/DTG thermogravimetric curves were obtained in a NETZSCH STA 409 C/CD apparatus with a 10 °C/min heating rate ranging from room temperature to 600 ºC under a nitrogen environment with a 60 mL/min flow rate, using alumina crucibles with masses between 14 and 20 mg for the pure chitosan and PEO (as received) samples and about 5 mg for the resulting electrospun blend membrane samples.

Differential Scanning Calorimetry (DSC)

The DSC curves were performed under a 50 mL/min N_2 flow rate in a DSC 2920 modulated apparatus from TA Instruments at a 10 °C/min heating rate and within a -100 to 250 °C temperature range using aluminum crucibles (top drilled) with approximately 5 mg sample masses. The curves were obtained by subjecting the specimens to a 10 ºC/min cooling rate to -100 ºC and kept at this temperature for 3 min. After that, the samples were heated at the same rate up to 250 °C, held isothermally for 3 min, and cooled again to -100 ºC at a 10 ºC/min rate and kept for 3 min before a new heating cycle up to 250 °C.

RESULTS AND DISCUSSION

Table 1 shows all prepared chitosan solutions, but not all of them could be processed. The most concentrated ones (6 and 7%) presented very high viscosities and the solution flow through the capillary was not possible. On the other hand, the less concentrated ones (1% and 2%) presented dripping through the capillary due to their low viscosities. Therefore, only the 4% concentration solution presented appropriate processing conditions for the equipment used in this work. Nevertheless, as reported by Klossner *et al*. (2008), who worked with chitosan (DD ≈ 80%) similar to that used in this study, it was not possible to obtain pure chitosan nanofibers, although different processing conditions were tested by varying the applied voltage and distance between the capillary and the collecting plate. However, in a previous study using the same solvent system (90% acetic acid in aqueous), Geng *et al*. (2005) reported obtaining pure chitosan nanofibers, while Klossner *et al*. (2008) linked these different results to the low chitosan DD (54%) used by Geng *et al*. (2005).

For the chitosan/PEO blends, fibers ranging from 50 to 300 nm in diameter were obtained (see Figs. 5 and 6).

Solution Characterization

The main solution properties that affect the electrospinning process are surface tension, electrical conductivity and rheological properties, which can be modified by the solution concentration and addition of salt. Figure 2 shows viscosity plots as a function of the shear rate for chitosan and chitosan/PEO solutions. Surface tension and electrical conductivity results are summarized in Table 3; these values are the averages of at least two measurements and did not differ by more than 0.2 mN/m for surface tension values and 0.1 μS/cm for electrical conductivity values.

Solution concentration is indicated by some authors (Ramakrishna *et al*., 2005; Klossner *et al*., 2008) as an important factor to control the formation of beaded structures in electrospinning, since the increase in the solution concentration will increase the solution viscosity. This increase is due to the increased polymer-chain entanglements in the solution (Hwang *et al*., 2000; Shenoy *et al*., 2005). It is expected that a certain degree of chain entanglement is present in the solution to avoid jet breakup during electrospinning. However, very high viscosities are not desirable, since they would avoid the formation of the jet during the process.

In the specific case of chitosan, solution concentrations of approximately 4-6% already present a gel structure leading to very high-viscosity solutions. The addition of a PEO solution (3%) to those solutions leads to lower viscosity, maintaining the total polymer concentration of the system.

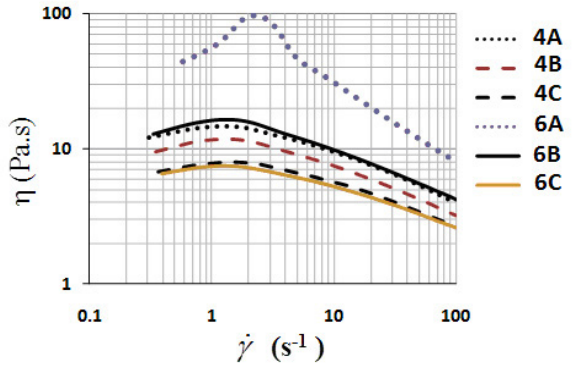

Figure 2: Viscosity plots as a function of the shear rate.

In Figure 2, it can be seen that all the solutions presented shear-thickening behavior at low shear rates and a power-law shear-thinning behavior at rates above 10 s^{-1}. Shear thickening is a characteristic rheological behavior of associative polymers (Barnes, 2000). Particularly, solution 6A showed substantial thickening due to its higher chitosan concentration. Shear thickening at low shear rates was also observed for chitosan/PEO blends. It can be seen that the addition of PEO to the solution caused an overall reduction in the solution viscosity. It can also be observed that, among the solutions with PEO analyzed, blends 4B, 4C, and 6C are the ones that presented the lowest viscosity values for the shear rate ranges analyzed and those blends presented good process capacity.

Furthermore, the addition of PEO led to a small reduction in the solution surface tension (see Table 3), which is desirable for electrospinning, since a fluid with a high surface tension tends to break into droplets during the process. By comparing the surface tension and conductivity values obtained for solutions 4B and 6C (both without salt) or 4C and 6D (both with salt), a lower surface tension and higher electrical conductivity in the blends prepared with solution 6A (with a higher chitosan concentration) can be observed (Table 3). Considering that the chitosan concentration in those solution blends is the same, i.e. 3%, those different properties should be attributed to the higher PEO concentrations in the systems.

Thus, the addition of PEO to chitosan solutions caused an increase in their electrical conductivity, which was already high for those chitosan solutions due to their cationic character, attributed to the presence of amine groups in the chitosan chains. As expected, the addition of salt resulted in a substantial increase of the solution electrical conductivity.

Electrospinning of the Blends and Membrane Obtainment

The difficulty to prepare HMW or MMW chitosan solutions of suitable concentrations and viscosities has been the main obstacle in chitosan electrospinning. However, this problem may be overcome using chitosan blends with biocompatible synthetic polymers (Klossner *et al*., 2008).

Regarding the polymer and solvent systems used in this work, it was observed that lower polymer solution viscosities and surface tensions led to more favorable processes. Thus, blends 6D, 4C and 6C showed better process capacity, followed by blend 4B.

The presence of NaCl in blend solution 4C showed an increase in its electrical conductivity when compared to the solution without salt (4B). It also caused a reduction in the blend's viscosity, while no significant changes were observed in the blend surface tension. Undoubtedly, the favorable

change in these two parameters, i.e., the large increase in conductivity and the viscosity reduction, ensured an easy and uninterrupted process. This same situation occurred during the processing of the 6C blend solution. It was processed again after the addition of salt (blend 6D, Table 3), also resulting in an easy process.

Although the addition of salt permitted an easier spinning process, it did not favor the formation of homogeneous membranes. An irregular spreading of the fibers was observed, forming very thin and inconsistent webs (Fig. 3, left). Figure 3 (right) shows pictures of a membrane obtained by processing blend 4B (blend without salt). There, a well-shaped membrane can be observed (a) immediately after processing, and (b) the same membrane being released from the mold. The latter was obtained with an electrospinning period of 4 hours and presented a thickness of approximately 150 μm.

The use of a rotating device between the capillary (containing the solution) and the collector enabled obtaining more consistent membranes. Figure 4a shows a picture of a membrane obtained using the rotating device with a period of 4 h spinning, resulting in a membrane with a thickness on the order of 100 μm. Further research with different rotating devices allowed the obtainment of other geometries, such as tubular geometries. An example that illustrates the versatility of the technique can be seen in Figure 4b, which shows a picture of a specimen supported in a needle in the vertical position and the inner diameter of the specimen lit by sunlight.

Table 3: Characterization of the blend solutions and pure chitosan solutions.

Blend solutions and pure chitosan solutions						Surface tension (mN/m)	Conductivity (mS/cm)
Sample		Chitosan/PEO*	NaCl** (%)	Chitosan %	Total polymer %		
4% Chitosan solution.	4A	3/0	0	4.0	4.0	43.9	1.13
	4B	3/1	0	3.0	3.75	42.5	1.71
	4C	3/1	1	3.0	3.75	42.7	5.21
6% Chitosan solution.	6A	2/0	0	6.0	6.0	58.0	1.53
	6B	2/1	0	4.0	5.0	50.8	2.54
	6C	2/2	0	3.0	4.5	41.9	2.41
	6D***	2/2	1	3.0	4.5	41.7	6.14

*PEO solution used: 3% in deionized water (w/v).
**% relative to chitosan solution.
***the same 6C blend (added salt after preparation).

Figure 3: On the left, a picture of the membrane made from the 6D-blend solution (with NaCl); on the right, the membrane made from blend 4B (without salt), a) picture taken immediately after the electrospinning process, b) releasing the membrane from the mold.

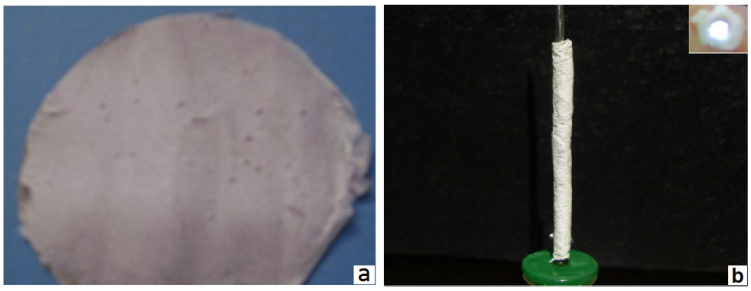

Figure 4: Blend 4B electrospun specimens obtained with the use of rotating devices; a) a 10 cm diameter membrane b) photo, in the vertical position, of a tubular-geometry specimen and a cross-sectional view (top right).

Morphological Characterization of the Membranes

In Figures 5 and 6, SEM images show the morphology of two highly porous nanostructured membranes made with blend 4B, as well as the fiber diameters which were determined from the image. These membranes were obtained using the basic electrospinning set up (see Figure 1a) and an applied voltage of 20 kV, keeping a distance from the tip of the needle to the collector plate of 9 and 7 cm respectively. These images show that the characteristic fiber diameter is in the order of 100 nm. Moreover, beaded structures were not observed.

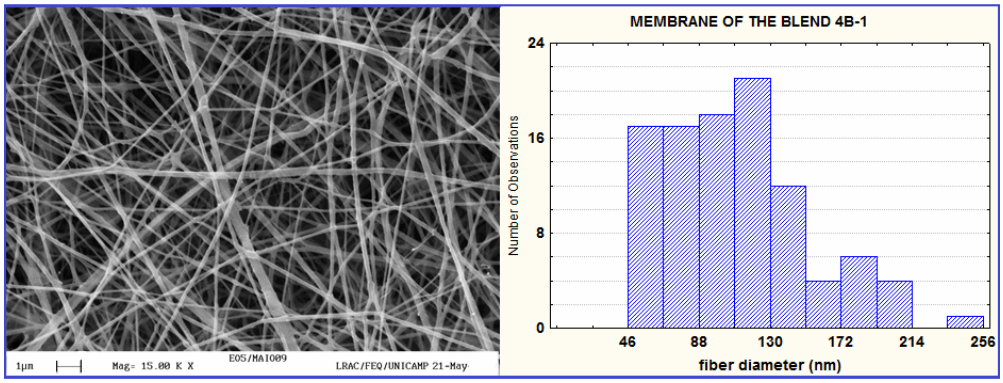

Figure 5: SEM image at 15,000-fold magnification and a representative histogram of the fiber diameter distribution of a membrane made with blend 4B produced with the basic equipment at an applied tension of 20 kV and a 9-cm distance between the needle tip and the collector plate.

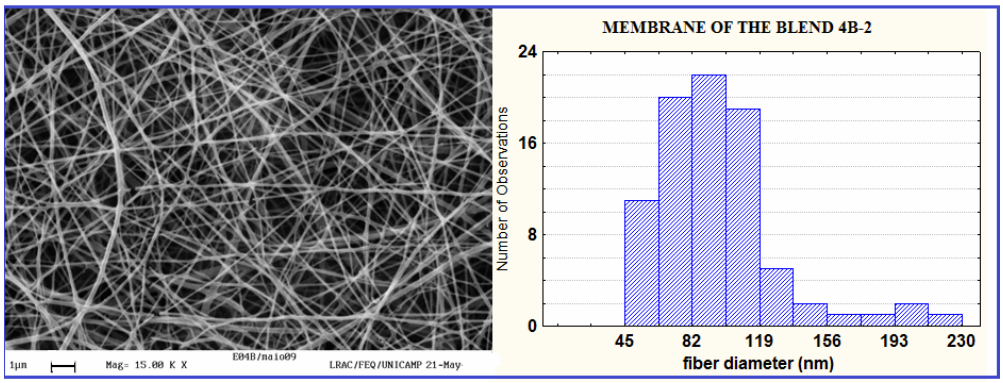

Figure 6: SEM image at 15,000-fold magnification and a representative histogram of the fiber diameter distribution of a membrane made with blend 4B produced with the basic equipment at an applied tension of 20 kV and a 7.5-cm distance between the needle tip and the collector plate.

With the use of a 32mm diameter rotating device, a smaller area occupied by the fibers deposited in the collector was observed. This was probably caused by the reduction in the diameter of the jet spiral during processing. Then, to obtain 10-cm diameter membranes with acceptable homogeneity, it was necessary to move the needle over the cylinder to increase the deposition area. SEM images and size diameter distribution of a membrane obtained using the rotating device can be seen in Figure 7**.** Table 4 summarizes the average diameters and standard deviations of the membrane-fibers obtained from blend solutions 4B using the basic electrospinning set up with a grounded aluminum plate as a collector (Fig. 1a) and also with a rotating device (Fig. 1b). It can be observed that the fibers of the membranes obtained with the use of the rotary collector showed a larger average diameter.

Membrane-Porosity Estimation

Samples of the membranes submitted to analysis by SEM showed images of fibers with diameters between the submicrometer and nanometer range, forming structures of highly porous non-woven webs. To estimate the porosity the liquid intrusion method was used, adapted to the methodology described by Soliman *et al.* (2010). The values obtained using this methodology comprise the average of three independent assays and are summarized in Table 5.

It can be observed that the porosity values obtained did not differ by more than 9%. The membrane from blend 4B, produced in the equipment with the rotating device (Fig. 1b) showed the highest porosity value (86%). However, the difference between this value and those presented by other

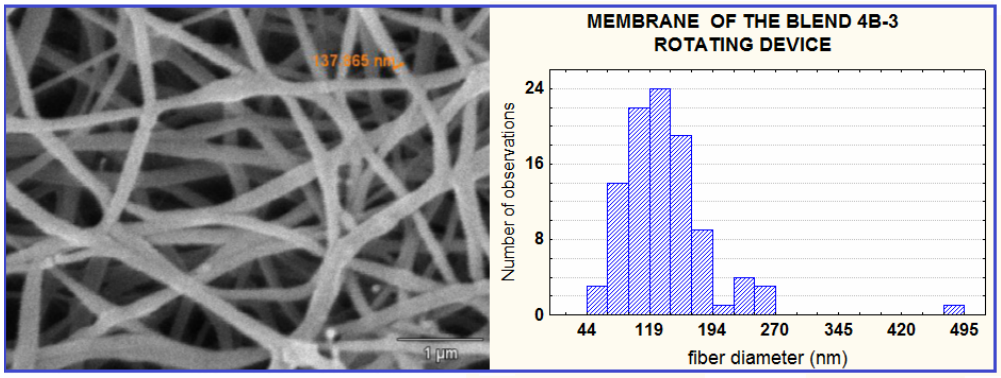

Figure 7: SEM image at 20,000-fold magnification and a representative histogram of the fiber diameter distribution of a 4B-formulation membrane obtained using the 32mm diameter rotating device.

Table 4: Average diameters and standard deviations of the fibers. Membranes obtained from blend solutions 4B.

Set up	Membrane	Average diameter (nm)	Measurements (n)
Basic (Figure: 1a)	(1)	111±42	100
Basic (Figure: 1a)	(2)	96±34	84
Rotating (Figure: 1b)	(3)	139±57	100

Table 5: Values of density and membrane porosity estimates.

Identification	Density (g/cm^3)	Porosity in free volume % (p)
4B Blend	0.839	81±4.2
4B Blend (obtained in rotating collector)	0.893	86±2.9
6C Blend	0.906	82±4.3
Ethyl alcohol	0.792	---

types of membranes does not exceed five percent, being therefore of the same order of magnitude as the analytical error observed. Moreover, the other types of membranes had p values that were very close in relation to the observed errors. The liquid intrusion assays confirm the high porosity of the membranes revealed by the SEM images.

Thermal Characterization

Figure 8 presents the TG/DTG curves for the pure chitosan (Fig. 08a) and pure PEO (Fig. 08b) samples, as well as for the sample obtained from the 4B-blend electrospun membranes prepared using the rotating device (Fig. 8c).

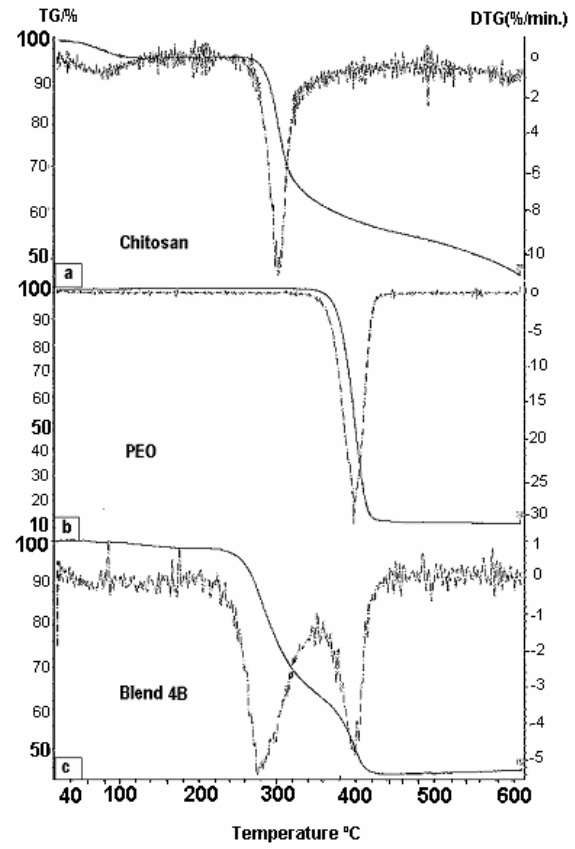

Figure 8: TG/DTG curves, a) pure chitosan; b) pure PEO and c) for the sample obtained from blend 4B electrospun membranes using the rotating device at 10 ºC/min.

Within the 20-610 °C temperature range, the chitosan sample presented two distinct mass-loss events: first, a broad event that extended from the beginning of the heating to 130 °C, with the maximum loss at around 80 ºC, corresponding to 5% the water loss and other possible volatile losses; the second mass loss refers to the depolymerization and degradation of chitosan, starting at about 260 ºC and showing a sharp peak at approximately 300 ºC.

In the case of PEO, a single mass-loss event was observed, corresponding to its decomposition, which begins at about 360 °C with the maximum peak at approximately 400 °C, reducing in intensity at around 420 ºC. After that, it remains almost stable until the end of the test (605 ºC), corresponding to a mass loss of about 89% of the sample. This final stability is probably due to the inert environment (nitrogen flow) in which the test was conducted. Finally, in the membrane TG/DTG thermograms resulting from blend 4B (chitosan/PEO), three thermal events can be observed: the first, almost imperceptible, is attributed to free and absorbed water and possible volatile loss between 60 and 130 °C. Despite the higher chitosan concentration (80%) in the final electrospun blend composition, the mass-loss percentage was below 2%. This suggests that the interactions between the chitosan/PEO chains and their orientation due to the great stretching during the electrospinning process (Na *et al*., 2008; Costa *et al*., 2009) caused a hydrophobic effect, avoiding water absorption.

In the second event, the mass loss corresponds to the chitosan decomposition temperature, which starts approximately 20-30 ºC earlier than that of pure chitosan. This behavior may be related to the possible chitosan molecular weight degradation during the electrospinning process. This phenomenon is under investigation by the group, including other polymers besides chitosan.

Finally, the third event, that began as expected before the end of the second, recorded a more intense mass loss at 400 °C, the same temperature as pure PEO.

The DSC curves for the same samples submitted to TG and for the 6C membrane sample electrospun using the rotating device are illustrated in Figures 9, 10 and 11. The data obtained for all thermal parameters are shown in Table 6.

The pure chitosan (Fig. 9) curve presented only one endothermic event, observed in the first heating, which corresponds to the dehydration of the saccharide rings in the polymer chains (Covas *et al*., 1993) and is also dependent on the drying or exposure history of the sample (Santos *et al*., 2003). This is confirmed by the absence of this event in the second heating (Fig. 11) and by the mass loss detected in the first thermal event presented in the TG/DTG analysis curves, as discussed earlier.

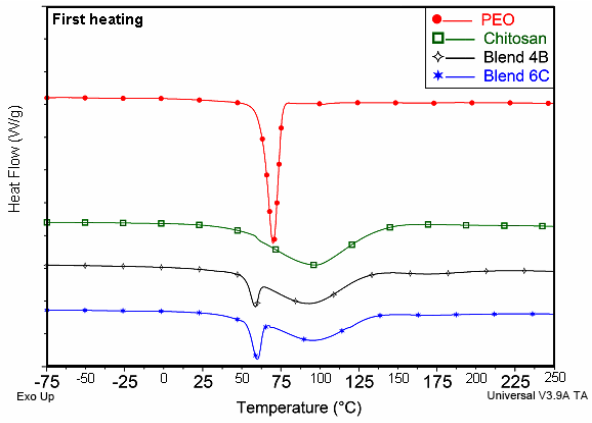

Figure 9: First heating DSC curves for pure chitosan and PEO powders and for membrane samples of blends 4B and 6C.

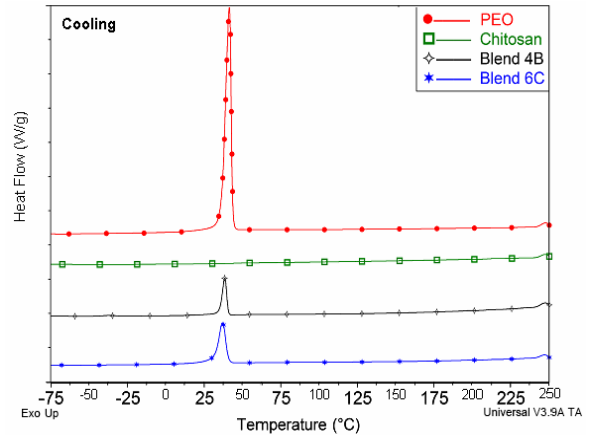

Figure 10: Cooling DSC curves for pure chitosan and PEO powders and the membrane samples of blends 4B and 6C.

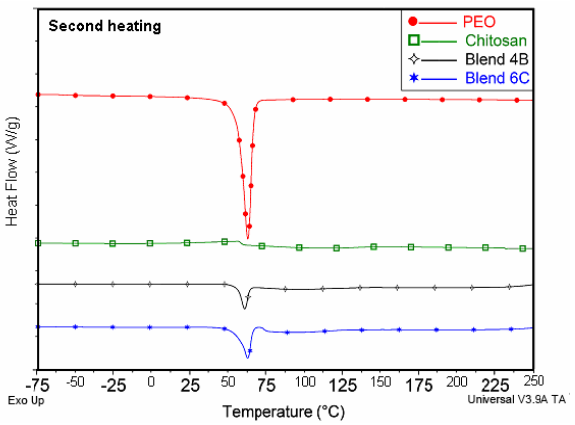

Figure 11: Second heating DSC curves for pure chitosan and PEO powders and for membrane samples of blends 4B and 6C.

Chitosan, like some other polysaccharides, suffers thermal degradation without melting, even under severe temperatures (Duan *et al*., 2004). With regards to pristine PEO, its melting temperature obtained in the first heating was around 71 °C, which is higher than that obtained in the second heating after the thermal history of the sample had been erased. However, even in the first heating, when chitosan is present, the PEO melting peak shifts to lower values (Fig. 9), clearly showing the interference of chitosan in the degree of PEO crystallinity. Furthermore, comparing the PEO crystallization temperatures (43.4 ºC) and those of the blends (38.5 e 37.0 ºC) in the cooling runs, it can be seen that the presence of chitosan disfavored and delayed the crystallization of the PEO.

Table 6: DSC and TG data for PEO/chitosan blends, pure PEO and chitosan powders.

Sample	DSC							TG			
	First heating			Cooling		Second heating		Water loss	Decomposition		
	T_m (ºC)	Dehyd (ºC)	ΔH (J/g)	T_c (ºC)	ΔH_c (J/g)	T_m (ºC)	ΔH_m (J/g)	Peak (ºC)	T_{onset} (ºC)	$Peak_1$ (ºC)	$Peak_2$ (ºC)
PEO as received	70.9		176.1	43.4	134.7	64.0	144.7		360	400	
Chitosan as received		96.8	311.6	---	---	---	---	80	260	300	
Blend 4B	59.2	92.0	62.3 176.3	38.5 ---	19.2 ---	60.5 ---	21.3 ---		≈235	≈280	400
Blend 6C	60.1	96.0	86.1 144.9	37.0 ---	33.2 ---	62.3 ---	31.9 ---				

CONCLUSIONS AND FUTURE WORK

An important achievement in this work was the production of submicron and nanosized fiber membranes with a high percentage (80%) of a biocompatible bioabsorbable antimicrobial polymer: chitosan. Through SEM images, the nanostructured morphology of the membranes was confirmed, as well as the presence of pores. The coupling of rotating devices to the basic electrospinning apparatus did not reduce the diameter of the fibers obtained, but enabled the preparation of membranes with a more consistent aspect and varied geometries. Although the thermal analysis results showed that the electrospinning process did not modify the thermal properties of the original polymers considerably, it was observed that the presence of chitosan interferes with PEO crystallization. The rheological study and the conductivity measurements of chitosan solutions and their solution blends clearly showed that the addition of PEO, as well as NaCl, favored the electrospinning process by reducing the viscosity and simultaneously increasing the electrical conductivity of the solutions.

Among the formulations that produced fibers with few defects, blend 4B was preferentially chosen to obtain the membranes due to its higher chitosan content.

The next step of this work was the development of *in vitro* tests, such as cytotoxicity, cell adhesion and cell growth, to evaluate the potential of the membranes to be used *in vivo*.

ACKNOWLEDGMENTS

The authors thank Dr. R. E. S. Bretas from DEMa-UFSCar for her help in the beginning of the project, Prof. L. A. Feijó. for assembling the high-voltage power supply, and Dr. W. Loh and Dr. E. Sabadini, from IQ-UNICAMP, who made their Labs and services available for the rheological characterization and measurements of the surface tension of polymer solutions and blends in solution, and the CNPq for the financial support (scholarship - p. 140146/2008-3).

REFERENCES

Barnes, H. A., A Handbook of Elementary Rheology. University of Wales, Institute of Non-Newtonian Fluid Mechanics, Aberystwyth (2000).

Costa, L. M. M., Bretas, R. E. S. and Gregorio Jr., R., Caracterização de filmes de PVDF-β obtidos por diferentes técnicas. Polim. Cienc. Tecnol., 19, No. 3, 189 (2009). (In Portuguese).

Covas, C. P., Monal, W. A. and Roman, J. S., A kinetic study of the thermal degradation of chitosan and a mercaptan derivative of chitosan. Polymer Degradation and Stability, 39, No. 1, 21 (1993).

Duan, B., Dong, C., Yuan, X. and Yao, K., Electrospinning of chitosan solutions in acetic acid with poly(ethylene oxide). J. Biomater. Sci., Polym. Edn., 15, No. 6, 797 (2004).

Geng, X., Kwon, O., and Jang, J., Electrospinning of chitosan dissolved in concentrated acetic acid solution. Biomaterials, 26, 5427 (2005).

Huang, Z. M., Zhang, Y. Z., Kotaki, M. and Ramakrishna, S., A review on polymer nanofibers by electrospinning and their applications in nanocomposites. Compos. Sci. Technol., 63, 2223 (2003).

Hwang, J. K. and Shin, H. H., Rheological properties of chitosan solutions. Korea-Australia Rheology Journal, 12, No. 3/4, 175 (2000).

Jayakumar, R., Prabaharan, M., Nair, S. V. and Tamura, H., Novel chitin and chitosan nanofibers in biomedical applications. Biotechnol. Adv., 28, 142 (2010).

Klossner, R. R., Queen, H. A., Coughlin, A. J. and Krause, W. E., Correlation of chitosan's rheological properties and its ability to electrospin. Biomacromolecules, 9, No. 10, 2947 (2008).

Kumbar, S. G., Nukavarapu, S. P., James, R., Hogan, M. V. and Laurencin, C. T., Recent patents on electrospun biomedical nanostructures: An overview. Recent Pat. Biomed. Eng., 1, 68 (2008).

Li, D., Ouyang, G., McCann, J. T. and Xia, Y., Collecting electrospun nanofibers with patterned electrodes. Nano Letters, 5, No. 5, 913 (2005).

Ma, Z., Kotaki, M., Inai, R. and Ramakrishna, S., Potential of nanofiber matrix as tissue-engineering scaffolds. Tissue Engineering, 11, 101 (2005).

Na, H., Zhao, Y., Zhao, C., Zhao, C. and Yuan, X., Effect of hot-press on electrospun poly(vinylidene fluoride) membranes. Polym. Eng. Sci., 48, No. 5, 934 (2008).

Petrulyte, S., Advanced textile materials and biopolymers in wound management. Dan. Med. Bull., 55, No. 1, 72 (2008).

Ramakrishna, S., Fujihara, K., Teo, W. E., Lim, T. C. and Ma, Z., An introduction to electrospinning and nanofibers. World Scientific, Singapore (2005).

Sajeev, U. S., Anand, K. A., Menon, D. and Nair, S., Control of nanostructures in PVA, PVA/chitosan blends and PCL through electrospinning. Bull. Mater. Sci., 31, No. 3, 343 (2008).

Santos, J. E., Soares, J. P. and Dockal, E. R., Caracterização de quitosanas comerciais de diferentes origens. Polim. Cienc. Tecnol., 13, No. 4, 242 (2003). (In Portuguese).

Schindler, M., Ahmed, I., Kamal, J., Nur-E-Kamal, A., Grafe, T. H., Chung, H. Y. and Meiners, S., A synthetic nanofibrillar matrix promotes in vivo-like organization and morphogenesis for cells in culture. Biomaterials, 26, 5624 (2005).

Shenoy, S. L. Bates, W. D., Frisch, H. L. and Wnek, G. E., Role of chain entanglements on fiber formation during electrospinning of polymer solutions: Good solvent, non-specific polymer–polymer interaction limit. Polymer, 46, No. 10, 3372 (2005).

Silva, H. S. R. C., Santos, K. S. C. R. and Ferreira, E. I., Quitosana: Derivados hidrossolúveis, aplicações farmacêuticas e avanços. Quim. Nova, 29, No. 4, 776 (2006). (In Portuguese).

Soliman, S., Pagliari, S., Rinaldi, A., Forte, G., Fiaccavento, R., Pagliari, F., Franzese, O., Minieri, M., Nardo, P. D., Licoccia, S., Traversa, E., Multiscale three-dimensional scaffolds for soft tissue engineering via multimodal electrospinning. Acta Biomaterialia, 6, 1227 (2010).

Teo, W. E. and Ramakrishna, S., A review on electrospinning design and nanofibre assemblies. Nanotechnology, 17, 89 (2006).

Wu, X., Wang, L. and Huang, Y., Application of electrospun ethyl cellulose fibers in drug release systems. Acta Polymerica Sinica, 2, 264 (2006).

Zhou, F. L. and Gong, R. H., Manufacturing technologies of polymeric nanofibres and nanofibre yarns. Polym. Int., 57, 837 (2008).